THE OFFICIAL MAGAZINE OF THE OCEANOGRAPHY SOCIETY

Oceanography

CITATION

Watt, S.F.L., P.J. Talling, and J.E. Hunt. 2014. New insights into the emplacement dynamics of volcanic island landslides. *Oceanography* 27(2):46–57, http://dx.doi.org/10.5670/oceanog.2014.39.

DOI

http://dx.doi.org/10.5670/oceanog.2014.39

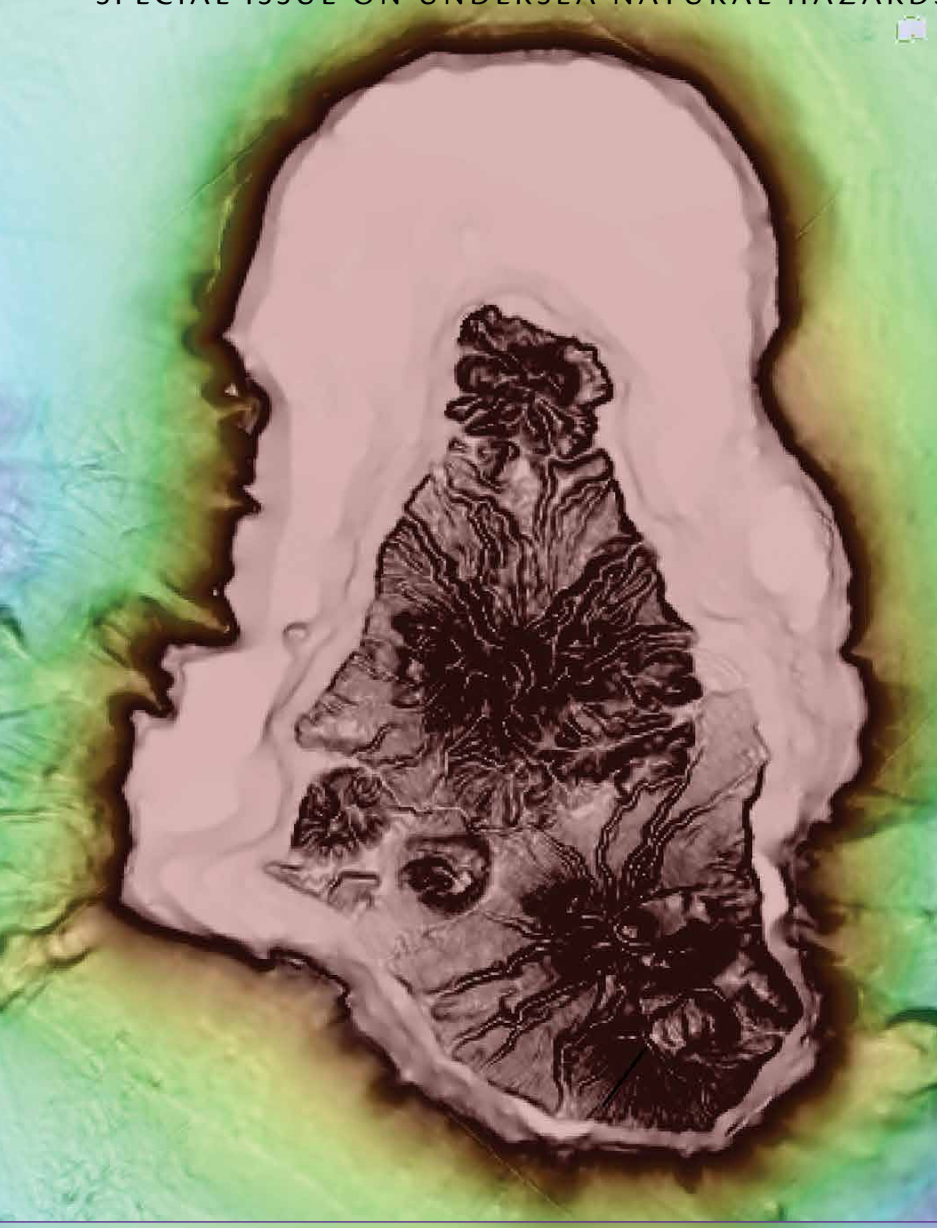

New Insights into the Emplacement Dynamics of Volcanic Island Landslides

BY SEBASTIAN F.L. WATT, PETER J. TALLING, AND JAMES E. HUNT

ABSTRACT. Volcanic islands form the highest topographic structures on Earth and are the sites of some of the planet's largest landslides. These landslides can rapidly mobilize hundreds of cubic kilometers of rock and sediment, and potentially generate destructive tsunamis on ocean-basin scales. The main unknown for tsunami hazard assessment is the way in which these landslides are emplaced. Understanding of landslide dynamics relies on interpretation of deposits from past events: it is necessary to understand where material within the deposit originated and the temporal sequence of the deposit's formation. The degree of fragmentation in a volcanic landslide is controlled by its relative proportions of dense lavas and weak pyroclastic rocks; fragmentation is generally reduced during subaqueous relative to subaerial transport. In the submarine environment, the seafloor-sediment substrate commonly fails during emplacement of a volcanic landslide. However, in many cases, this sediment failure remains almost in situ as a deformed package rather than disaggregating to form a debris flow. Because seafloor sediment makes up a large proportion of many landslide deposits around volcanic islands, the magnitude of the primary volcanic failure cannot be readily assessed without a clear understanding of deposit constituents. Both the dimensions of the volcanic failure and the way in which it fails are of key importance for tsunami generation. Turbidite deposits suggest that some volcanic landslides occur in multiple retrogressive stages. This significantly reduces potential tsunami magnitude relative to models that assume emplacement of the landslide in a single stage.

INTRODUCTION

Landslides derived from the flanks of volcanic islands are among the largest on Earth. They may transport hundreds or even thousands of cubic kilometers of material (Moore et al., 1989; Masson et al., 2002), dwarfing landslides from subaerial volcanoes, such as the 2.5 km^3 event that initiated the eruption of Mount St. Helens in 1980 (Glicken, 1996). Volcanic islands provide the greatest relief on our planet. For example, the peaks of the Canary Islands lie up to 7 km above the surrounding seafloor, with gradients of > 10° sustained for tens of kilometers on the island flanks.

Volcanic landslides themselves pose substantial hazards, and they may trigger explosive volcanic eruptions (Siebert, 1984; Glicken, 1996). In island or coastal settings, the largest landslides may generate destructive tsunamis on oceanic scales (Løvholt et al., 2008). Even relatively small (<1 km^3) events can trigger locally destructive tsunamis (Nishimura, 2008). Landslides may also induce decompression of subsurface magma storage systems and thus alter future eruptive behavior (Manconi et al., 2009; Pinel and Albino, 2013). A range of processes may trigger volcanic landslides (McGuire, 1996), including changes in sea level; thus, landslide frequency may be temporally variable (e.g., Boulesteix et al., 2012). The few direct observations of volcanic island landslide processes are limited to small, historical events (e.g., Stromboli; Tinti et al., 2006). Models of pre-failure conditions, triggering processes, and emplacement dynamics of large volcanic island landslides remain poorly validated.

The tsunami hazard from volcanic island landslides is well illustrated by three historical examples from Japan (Nishimura, 2008). A landslide at Komagatake in 1640 deposited ~ 1 km^3 of material underwater, with the resultant tsunami claiming 700 lives. A similar landslide at Oshima-Oshima in 1741 generated a tsunami that killed 2,000 people. Even more devastating, with 15,000 fatalities, was the 0.48 km^3 collapse at Mt. Unzen in 1792. All of these landslides were produced at subaerial volcanoes, and only part of each landslide entered the water. Much larger (> 100 km^3) events that incorporate material from both subaerial and submerged volcanic flanks are documented around many volcanic islands. There are few historical cases of landslides that resulted in entirely submarine deposits, but a good example is that at Ritter Island, Papua New Guinea, in 1888, which removed 5 km^3 of the volcanic edifice (Silver et al., 2009).

Modeling suggests that the largest-volume (> 100 km^3) volcanic-island landslides can generate tsunamis that travel across ocean basins (Løvholt et al., 2008). For instance, a worst-case-scenario, single-stage landslide on the Canary Islands may form tsunami wave heights of 3–8 m, before runup, along the east coast of North America (Løvholt et al., 2008). Landslides generate tsunamis through water displacement, both as they enter the ocean and as they move on the seafloor. Accurate modeling of tsunami generation requires a clear understanding of landslide failure and emplacement processes. Of particular importance to modeling are the total volume of the landslide, where this material originates (e.g., on the subaerial or submerged flanks), and whether this material is mobilized in single or multiple stages (Watt et al., 2012a). The magnitude of water displacement and the efficiency of wave generation depend on landslide volume, velocity, and water depth. There are very few observations that constrain landslide velocity, but a maximum estimate of 40–80 m s^{-1} for the Ritter Island landslide (Ward and Day, 2003) is similar to estimated velocities of subaerial volcanic debris avalanches (Glicken, 1996). For submerged landslides, efficient tsunami generation occurs when the landslide velocity is close to that of the tsunami wave (Ward, 2001), but subaerial slides entering the water may generate even larger waves if they move at higher velocities, piling water ahead of the landslide mass (Fritz et al., 2004). For landslides on volcanic island flanks, the early stages of movement are most important for tsunami generation, before the material spreads and decelerates (see Watt et al., 2012a).

The historical landslides described above all occurred in subduction zone settings. The largest landslides in these settings have volumes of tens of cubic kilometers (e.g., Deplus et al., 2001; Montanaro and Beget, 2011). Larger volcanic islands form in intraplate settings, associated with mantle plumes (e.g., Hawaii, Canary Islands) and are the sources of the largest volcanic-island landslides, reaching volumes of several hundred cubic kilometers (Moore et al., 1989; Masson et al., 2002). Landslide deposits across these different regions

OPPOSITE | The volcanic island of Montserrat, in the Caribbean, is seen at the top left, with a prominent eroded shelf. Shallowly submerged and subaerial topography is shaded as brown colors, with purple colors marking the deepest surfaces. Offshore the southeast corner of Montserrat, fields of blocky debris mark the surface of large landslide deposits derived from the slopes of the Soufrière Hills volcano. These landslides traveled into the basin at the bottom right, which is flanked by small seamounts.

BOX 1. TERMINOLOGY

Landslide is a general term for slope failure and the resulting mass movement. Following earlier work (Moore et al., 1989; Masson et al., 2002), volcanic island landslides are subdivided into *slumps* and *debris avalanches*. ***Slumps*** potentially involve multiple discrete fault-bound movements over a prolonged period, with deep basal décollements (gliding planes between two rock masses), and are associated with gradual deformation of the volcanic structure (e.g., Delcamp et al., 2008). We do not consider slumps further in this paper. The landslide deposits described here originate as *debris avalanches* on the volcanic edifice. ***Debris avalanches*** are deposited in discrete landslide events that affect relatively elongate areas, and they transport cohesionless rock fragments between clearly defined source and depositional regions. Landslide processes affecting the sedimentary cover around volcanic islands may be described as *slides* or *debris flows*. ***Slides*** involve the movement of coherent sediment masses bound by distinct failure planes. ***Debris flows*** transport disaggregated sediment as cohesive flows of clasts in a fine-grained matrix (Iverson, 1997). Debris avalanches with a high proportion of fine-grained material may develop elements of cohesive flow and can be considered coarse-grained debris flows (Masson et al., 2002). There is thus a continuum between these end-member types, and because no strict division can be defined, we follow Masson et al. (2002) in collectively referring to blocky deposits derived from the volcanic edifice as debris-avalanche deposits. Here, we also distinguish between ***volcanic edifice material*** and associated failures of pre-existing ***seafloor sediment*** beyond or mantling the base of the volcanic island flanks. ***Turbidity currents*** are dilute and highly mobile submarine sediment flows generated by mixing between landslides and surrounding seawater (Talling et al., 2012).

have similar physical characteristics, which are also shared with entirely subaerial volcanic landslide deposits (Siebert, 1984), suggesting that common processes control volcano instability and landslide behavior across all settings. Nevertheless, the extreme scale of some volcanic island landslides, and the influence of water and marine sediment on their emplacement mechanics, sets them apart from their subaerial equivalents.

Our understanding of volcanic island landslides relies mainly on the interpretation of scars and deposits from past events. Collapse scars provide information on landslide material and volumes but may be obscured by later volcanism. The majority of the landslide material is usually deposited on the seafloor, and structures within these deposits provide detailed information on the dynamics of landslide failure and emplacement. Seafloor mapping (e.g., side-scan sonar, swath bathymetry, submersible observations), seismic reflection imaging, and direct sampling (e.g., via sediment cores) provide the data for understanding these deposits. The sometimes extreme dimensions of these landslide deposits, which may cover thousands of square kilometers in water depths of several kilometers, can hinder high-resolution or comprehensive observations. Seismic reflection imaging of landslide deposit basal surfaces or internal structures is challenging due to their heterogeneous and coarse-grained nature. Nevertheless, seafloor imaging shows that landslide deposits occur at all types of oceanic volcanoes (e.g., Deplus et al., 2001; Mitchell, 2003; Coombs et al., 2007). It is clear that submarine landslides play a major role in volcanic island evolution, and that they are volumetrically important for global sediment transport (cf. Talling et al., 2012).

Our objective in this paper is to bring together a range of recent morphological, structural, and sedimentological observations that enhance our understanding of how landslide deposits around volcanic islands were emplaced. These observations show that depositional processes of volcanic island landslides are complex, often involving multiple stages and incorporating different types of material.

The first part of the paper describes the morphology of landslide deposits around volcanic islands. We show that morphology reflects emplacement processes and discuss the controls on material fragmentation and landslide mobility. The second part outlines how the rapid emplacement of volcanic landslides can trigger failure of pre-existing seafloor sediment. Such secondary failures are widespread, and we discuss their origin and propagation. We then consider evidence for how the failed mass is mobilized and whether it moves in single or multiple stages. Finally, we summarize the implications of the preceding sections for tsunami hazards.

Previous reviews of volcanic-island landslides generally focus on

Sebastian F.L. Watt *(s.watt@bham.ac.uk) is NERC Research Fellow, School of Geography, Earth and Environmental Sciences, University of Birmingham, Edgbaston, Birmingham, UK.* **Peter J. Talling** *is Leader, Geohazards and Sedimentology Research Group, National Oceanography Centre, Southampton, UK.* **James E. Hunt** *is Postdoctoral Researcher, National Oceanography Centre, Southampton, UK.*

well-studied groups of islands (e.g., Moore et al., 1989; Deplus et al., 2001; Masson et al., 2002; Silver et al., 2009; Montanaro and Beget, 2012; Hunt et al., 2013a), often with an additional aim of documenting all known landslide deposits in those geographic regions. Here, we bring together a range of insights from these earlier studies and also summarize recent results from detailed geophysical (e.g., Watt et al., 2012b) and sedimentological (e.g., Hunt et al., 2011, 2013b) studies of volcanic island landslide deposits. It is timely to collate these results, given that advanced geophysical capabilities and new methods of direct sampling can now help to address key questions regarding submarine landslide processes. A clearer understanding of these processes will enable development of a new generation of accurate models for landslide-generated tsunamis.

EMPLACEMENT OF MATERIAL FROM THE VOLCANIC EDIFICE

Figure 1 shows the shapes of collapse scars and submarine debris-avalanche deposits for various volcanic island examples. Morphologically, these scars and deposits are broadly comparable to their subaerial counterparts (e.g., Siebert, 1984). They have clearly defined headwalls, source-region scars, and chutes incised within volcanic topography, and they produce dispersed, blocky, and heterogeneous deposits beyond these flanks.

The very largest subaerial landslides, such as those at Socompa and Shasta volcanoes (Crandell, 1989; Wadge et al., 1995), mobilized up to 50 km^3 of volcanic rock. These events encompassed the edifice summit and removed sectors spanning as much as one-third of the volcano circumference. They also cut deeply toward the basement rock and removed at least 15–20% of the entire volcanic structure. Although landslides around volcanic islands may be far larger, they may also be more superficial in terms of the modifications they cause to their parental volcanic structures. This is due to the extremely large scale of some volcanic ocean islands relative to most subaerial volcanoes (Figure 2). For example, the Icod landslide, from Tenerife (Figure 1), transported > 250 km^3 of volcanic material (Hunt et al., 2011, 2013a), but its scar is a parallel-edged and relatively shallow feature (compared to the island basement), confined to one flank of Tenerife. The Icod event removed ~ 1% of the volume of Tenerife, which has a basal diameter of ~ 100 km. In contrast, the 5 km^3 Ritter Island landslide of 1888 removed ~15% of the volcanic structure of a much smaller island arc volcano.

Landslides that account for a large

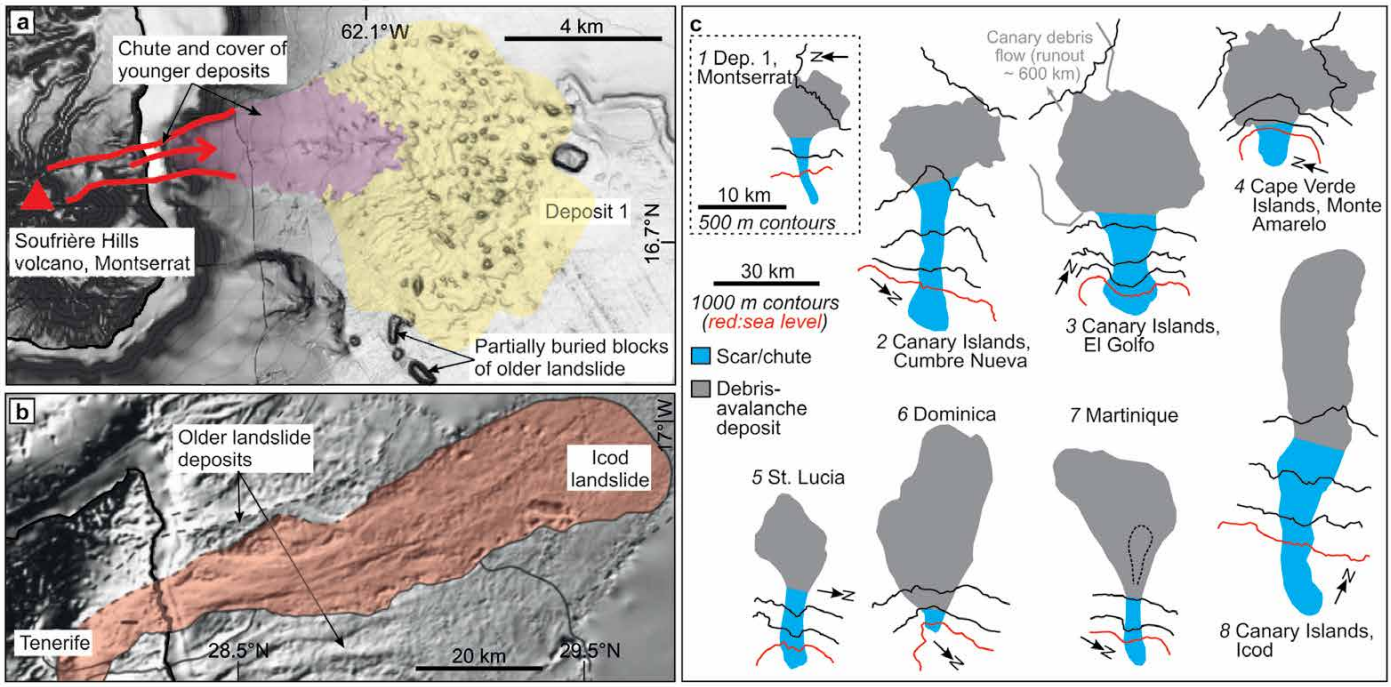

Figure 1. Shaded topographic gradient maps of (a) the Deposit 1 debris-avalanche deposit offshore Montserrat (Caribbean), a typical fan-shaped deposit with scattered blocks, and (b) the Icod debris-avalanche deposit offshore Tenerife, Canary Islands (Masson et al., 2002), an elongate deposit with linear surface features indicative of cohesive flow. (c) Shapes of selected volcanic island debris-avalanche deposits, differentiating the source (island flanks) and depositional (surrounding seafloor) regions (Deplus et al., 2001; Masson et al., 2002, 2008; Watt et al., 2012b). Deposits are ordered by increasing downslope length-to-width ratios.

proportion of the overall volcanic structure, regardless of their absolute volume, typically produce deep-seated and divergent scars that encompass the volcano summit (Figure 2). However, the broad profile of many intraplate volcanic islands may favor relatively shallow, parallel-sided source regions for debris avalanches. Instabilities that cut deeply into intraplate islands may form slumps (see Moore et al., 1989), but may not always develop into more mobile landslides, as they might on the steeper volcanic structures that predominate in subduction zone settings.

Material Fragmentation

Regardless of differences in magnitude, the morphological features of volcanic debris-avalanche deposits are broadly similar across all volcanic settings. However, what differentiates all the examples in Figure 1 from subaerial volcanic debris avalanches (Siebert, 1984) is that they contain some material sourced from and transported in an aqueous environment. In the submarine environment, the density contrast between the landslide material and the ambient fluid is much lower than for subaerial debris avalanches, and this difference may reduce both the degree of material fragmentation and the acceleration of the landslide.

There are clear morphological differences between the coarsest-grained components of subaerial and submarine debris-avalanche deposits. Blocks in submarine debris-avalanche deposits are formed via initial fragmentation near their source regions and may encounter only limited further interblock collision and fragmentation during transport. The most block-rich volcanic island landslides, such as El Golfo (Figure 2) or Nuuanu, Hawaii (Moore and Clague, 2002), are dominated by kilometer-scale blocks with steep sides and angular forms, which are essentially intact fragments of volcanic edifices that have slid to their site of deposition. Although intact blocks are observed in subaerial settings, they tend to be limited to the failure region (Figure 2). Within the main debris-avalanche deposit, subaerial deposits are dominated by large hummocks that have rounded forms and are composed of multiple fragments (Siebert, 1984; Crandell, 1989; Glicken, 1996). The dominance of angular, intact blocks in some submarine debris-avalanche deposits suggests a relative damping of fragmentation in the submarine environment (e.g., Mazzanti and De Blasio, 2013). Reduced fragmentation results from the lower density contrast between the landslide material and water, relative to air, which reduces the energy of intergrain interactions. The typically lower roughness and strength of the seafloor substrate in submarine settings may also inhibit fragmentation. In general, lower levels of fragmentation produce a coarser total grain-size distribution for landslide deposits. However, as we note below, the production of the fine grain sizes that are critical for cohesive landslide behavior is ultimately related to the strength of the failed volcanic material.

Mobility

The elongation of blocky debris-avalanche deposits is indicative of landslide mobility. This mobility directly reflects the material properties of the landslide (Masson et al., 2002). The examples in Figure 1 all spread, without topographic confinement, at the bases of the volcanic island flanks, and they are ordered in terms of increasing mobility, formalized as the ratio of a deposit's lateral spread to its extent in the direction of failure (Figure 3a). Block-dominated debris avalanches (i.e., the idealized cohesionless endmember) form fan-shaped deposits that result from radial spreading. For example, the El Golfo debris-avalanche deposit is composed of

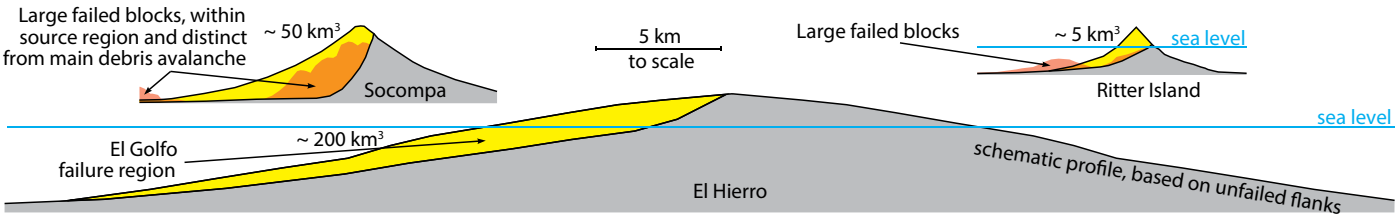

Figure 2. Scale cross sections (without vertical exaggeration) through volcanoes affected by large landslides. Socompa (Chile/Argentina border) is one of the largest known subaerial volcanic landslides. Its notably deep-seated nature means that many large blocks remain within the landslide scar region (Wadge et al., 1995). The smaller Ritter Island (~ 100 km northeast of New Guinea) collapse of 1888 (Ward and Day, 2003) was morphologically comparable. Both Socompa and Ritter are composite volcanoes formed in subduction zone settings. The much larger structure of El Hierro in the Canary Islands (Masson et al., 2002) is typical of an oceanic intraplate volcanic island. Its mean slope gradient is lower, but its large dimensions mean that even relatively surficial landslides have extremely large volumes. Parts of the cross sections (including pre-failure surfaces) are conjectural, due to later modifications of the volcanic edifice by volcanic eruptions and erosion.

a structureless spray of scattered blocks. In between the blocks, it is unclear how much material is derived from the volcanic flank failure. In contrast, elongated deposits such as Icod show clear evidence of downslope cohesive flow (Figure 1b). Although the Icod deposit displays numerous blocks on the surface, its overall appearance is mounded and banked (Ablay and Hürlimann, 2000), comparable to the similarly elongate deposits offshore the southern Lesser Antilles (Figure 4b). The size of individual blocks in the Icod deposit is far smaller than those at El Golfo, except for some marginal blocks rafted at the head of the landslide. These blocks indicate that the Icod landslide began as a block-dominated debris avalanche that acquired the characteristics of a cohesive debris flow during transport, via rapid and efficient material fragmentation (Masson et al., 2002).

The shape and texture of debris-avalanche deposits reflect the physical properties of the landslide constituents. High proportions of fine-grained material allow the landslide to develop internal pore pressures that enhance mobility (Iverson, 1997; Masson et al., 2002). Fine-grained material may also limit landslide permeability and facilitate hydroplaning (Mazzanti and De Blasio, 2013). Fine grain sizes may be acquired via volcanic rock fragmentation or by seafloor sediment incorporation. However, we suggest that the presence of easily fragmented, weak volcanic rock in the source region is fundamental to forming deposits with cohesive flow behavior, as revealed by comparing the Icod and El Golfo deposits. The El Golfo debris avalanche was emplaced on poorly consolidated, fine-grained seafloor sediment, and triggered the failure of this sediment to generate the Canary debris flow (Roberts and Cramp, 1996; Masson et al., 1998). Clearly, abundant fine-grained material was present on the seafloor, but it was not efficiently incorporated within the debris avalanche itself. The morphology of the El Golfo deposit does not show any evidence for cohesive flow (although we note that some fine-grained material must have been produced during the landslide to form the associated turbidite deposit [Hunt et al., 2013b], but perhaps in insufficient proportions to act as a matrix that could transport larger blocks). The block-rich nature of the El Golfo deposit is consistent with the volcanic geology of El Hierro, the source of the avalanche, which is dominated by dense lavas.

In contrast to El Golfo, the Icod source region includes substantial proportions of much weaker pyroclastic deposits interbedded with lavas. This pyroclastic rock may rapidly fragment during transport to produce sand- and mud-grade material that forms a cohesive matrix and potentially enhances further incorporation of erodible seafloor sediment. It is thus the nature of the volcanic landslide material, rather than simply the degree of fragmentation, that is a key influence on mobility (Masson et al., 2002).

As discussed above, fragmentation may be higher overall for subaerial volcanic debris avalanches than in their submarine equivalents. However, if dense lavas dominate the initial geology, fragmentation is still unlikely to generate large proportions of fine-grained sediment. Thus, a subaerial analogue for El Hierro may be the debris-avalanche deposit at Jocotitlán, Mexico (Siebe et al., 1992), where conical hummocks of dense lava cobbles replace the scattered blocks. The dominant grain size at Jocotitlán is on a decimeter scale, and there is very little fine material. Similarly, the presence of an erodible substrate is not required to produce an elongate, mobile deposit; more important is the presence of weak and friable volcanic rock, such as in the pumice-dominated but entirely dry flank-collapse deposit at Lastarria, Chile (Naranjo and Francis, 1987).

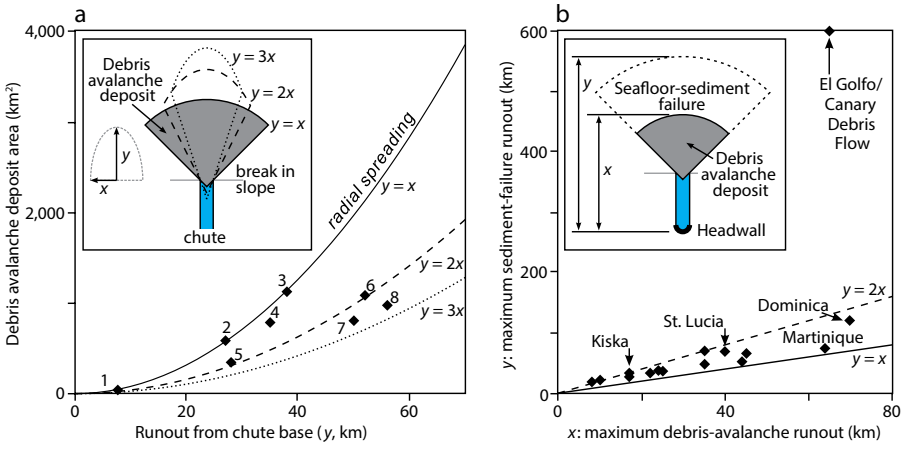

Figure 3. (a) Debris-avalanche deposit area against downslope extent for the deposits numbered in Figure 1. Continuous lines show the area-extent relationship defined for different ratios of lateral to downslope deposit spreading (see inset). Fan-shaped deposits ($y = x$) correspond to debris avalanches dominated by large blocks, while elongate deposits show evidence of a significant fine-grained component. (b) Runout distances for debris-avalanche deposits and the failures of seafloor sediment triggered by their emplacement (see inset). In most cases, the extent of seafloor sediment failure is relatively limited in comparison to the mobility expected for a debris flow (note the Canary debris flow point). This is consistent with the confined nature of these sediment failures.

SECONDARY FAILURE OF SEAFLOOR SEDIMENT

As a volcanic debris-avalanche is transported through the submarine environment, fine-grained material mixes with seawater to form turbidity currents that transport sediment into surrounding ocean basins (e.g. Hunt et al., 2011). The deposits of these flows (turbidites) provide important information on landslide emplacement. Landslide emplacement on the seafloor will also load the underlying substrate of water-saturated sediment, and this material may become incorporated within the final landslide deposit.

There is good evidence that seafloor sediment can be disrupted to depths of >100 m by debris avalanche emplacement (Figure 4), both by basal erosion and by the induced failure of loaded sediment (Watt et al., 2012a,b). We first consider surface morphological features that indicate such processes, and then interpret them in the light of internal structures.

Surface and Internal Characteristics

In several instances, submarine volcanic debris-avalanche deposits are surrounded by smoother-surfaced regions of seafloor (Figure 4) that are marked by small scattered blocks or marginal banks, indicating that they form part of a landslide deposit (e.g., Deplus et al., 2001; Silver et al., 2009; Montanaro and Beget, 2011). These smooth-surfaced deposits could be interpreted as partially buried, older landslide deposits, smoothed by a younger sedimentary cover (Deplus et al., 2001). However, there is no difference in the thickness of post-emplacement sedimentary cover between the blocky and smooth-surfaced regions at these sites, suggesting that the two were formed contemporaneously (Watt et al., 2012a). An alternative explanation is that the smooth-surfaced areas represent finer-grained debris-flow deposits triggered by emplacement of the volcanic debris avalanche (Silver et al., 2009). This interpretation is also problematic because of the limited extent of the smooth-surfaced regions. Debris flows are slurries of disaggregated, highly mobile clasts exhibiting a cohesive behavior. The extent of the smooth-surfaced regions around many submarine volcanic debris avalanches is of the same order as that of the blocky region (Figure 3b) and is, therefore, inconsistent with a debris-flow origin. The runout of debris flows is far greater, as shown by the example of the Canary debris flow, which was triggered by the El Golfo debris avalanche (Figure 3b). A debris-flow origin is also countered by the fact that these smooth-surfaced regions are not clearly associated with a headwall (marking a region where sediment was removed). Rather, they have a geometry that radiates out from the internal, blocky deposit.

Seismic reflection profiles reveal the true origin of the smooth-surfaced regions observed around many submarine debris-avalanche deposits, showing that they mark zones of disruption within pre-existing seafloor stratigraphy. The outer margins of these disrupted stratigraphic packages are confined and truncate against undisturbed

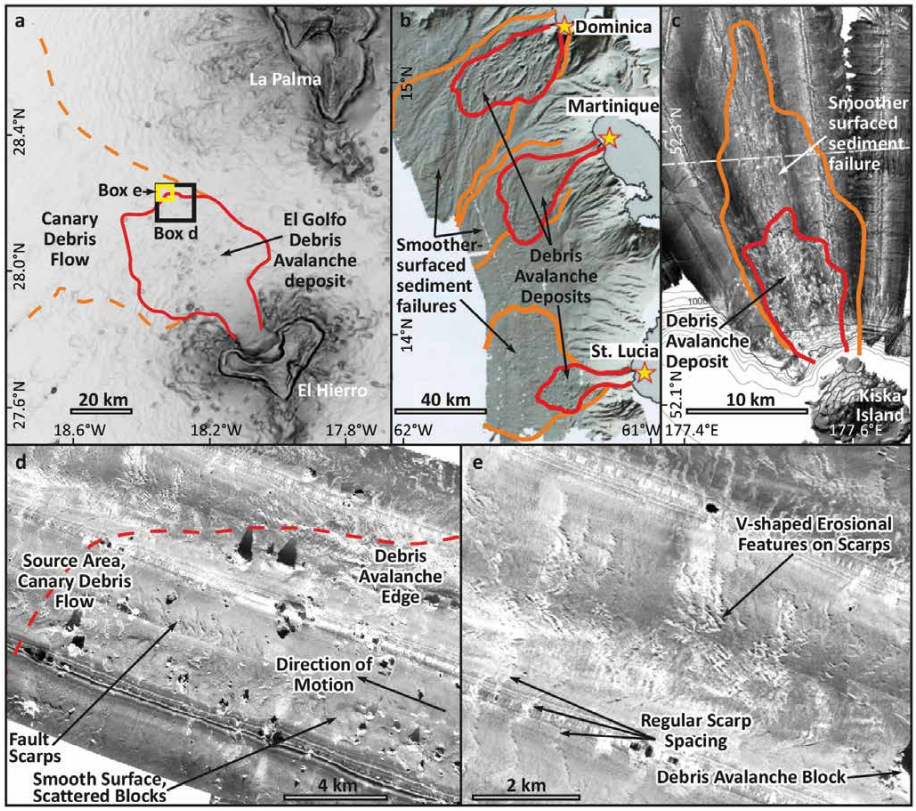

Figure 4. Volcanic island landslide deposits where debris-avalanche deposition is associated with seafloor sediment failure. Shaded bathymetry of the (a) El Golfo debris avalanche, associated with triggering the Canary debris flow (Masson et al., 1998), and (b) debris avalanches in the southern Lesser Antilles (Deplus et al., 2001; Le Friant et al., 2003), where blocky deposits are associated with smoother-surfaced seafloor sediment failures. Side-scan sonar images of (c) a similar deposit at Kiska Island, Aleutian arc (Coombs et al., 2007), and the (d) edge of the El Golfo deposit, showing scattered blocks and extensional fault ridges in the source region of the Canary debris flow (Masson et al., 1998). (e) Detail of fault scarps in (d).

beds of seafloor sediment. Internal structures, described below, show that these disrupted bodies of sediment are not formed by material disaggregation or downslope transport (i.e., between source and depositional regions), but rather form via in situ deformation. The terminology of *flow*, or even of *slide*, is therefore inappropriate for these portions of submarine volcanic island landslides. Here, we refer to them as *confined seafloor sediment failures*, following the frontally confined landslide terminology used by Frey-Martínez et al. (2006) to describe similar units. The term *confined* emphasizes that the deforming seafloor sediment did not form a mobile flow.

The seismic reflection profile in Figure 5A shows a landslide deposit offshore Montserrat (Watt et al., 2012b). It provides good evidence that blocky debris avalanches can incise deeply into poorly consolidated seafloor sediment. In the case shown, large blocks are imaged within a deposit that cuts approximately 100 m down into the underlying beds of seafloor sediment. Truncated sediment beds show that this material has been removed and incorporated into the landslide deposit. The seismic characteristics of this proximal volcanic landslide deposit are typical, with an irregular top surface and a structureless interior.

In Figure 5B, a seismic reflection profile through the landslide margin shows very different structures. This is a region of confined seafloor sediment failure, associated with upslope debris-avalanche emplacement (Watt et al., 2012b). Here, volcanic blocks are absent. The deposit base follows single stratigraphic horizons for long distances, with occasional steps, and has a relatively smooth upper surface. Internally, there is patchy preservation of bedding. In some cases, bedding appears fully intact and is indistinguishable from the sediment beds above and below. Elsewhere, the bedding is lightly folded, and there are internal thrusts at the confined toe of the landslide. There is no clear deposition above the paleo-topographic surface except for a relatively thin overriding deposit. Rather, the landslide stops against the equivalent, undisturbed sediment beds, illustrating its confinement. Seismic reflection profiles at the margins of other Lesser Antilles landslides (Figure 4b) show the same features (Watt et al., 2012a) of a landslide base following a sediment stratigraphic horizon, with hints of internal bed structures, and of a margin that truncates against undeformed sediment.

The confined seafloor sediment failures described here involve widespread deformation of a package of seafloor sediment. This deformation is compressional, as indicated by the internal folding, but the overall amount of downslope transport is small; the material does not disaggregate, and there is no clear sense of a source or depositional region. These failures also have limited surface topographic expression and lie mostly beneath the pre-landslide seafloor surface.

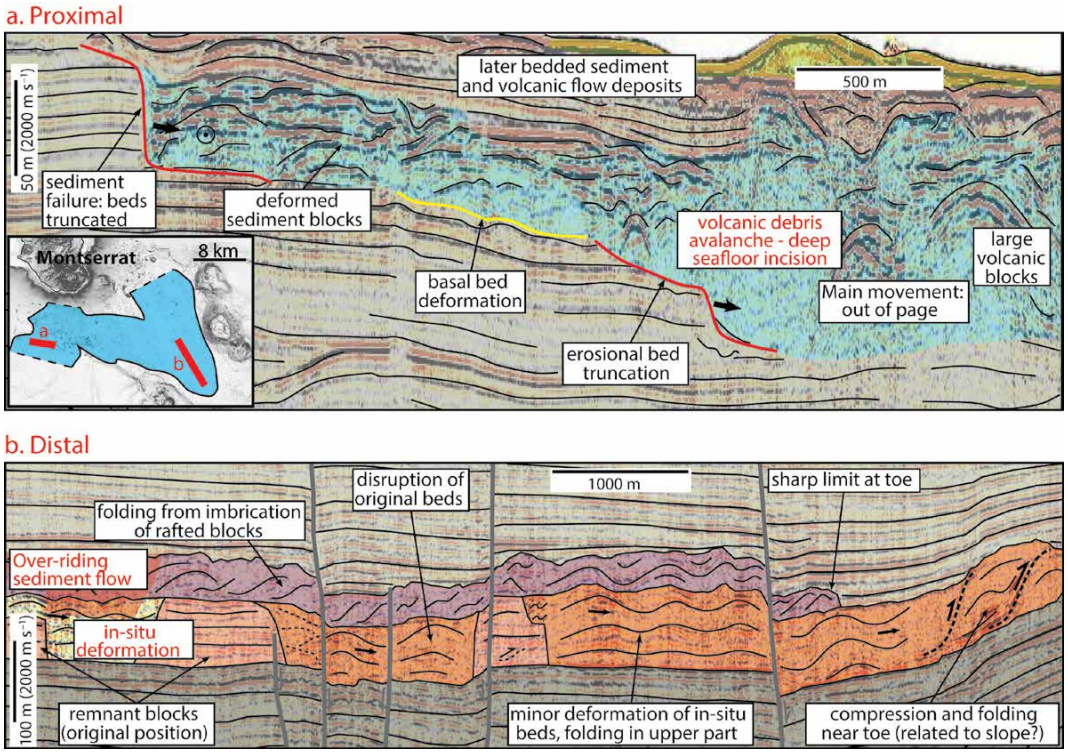

Figure 5. (a) Proximal seismic reflection profile across the Deposit 4 landslide deposit offshore Montserrat, highlighting the incision into well-bedded seafloor sediment by a blocky, heterogeneous volcanic debris avalanche. (b) Distal seismic reflection profile along the associated Deposit 8, interpreted as the seafloor sediment failure triggered by Deposit 4 (Watt et al., 2012b). This deposit contains no large volcanic blocks and has a base that follows stratigraphic horizons. No evacuation occurs at the landslide toe; sediment failure is characterized by distributed deformation within a confined body.

Mechanisms of Seafloor Sediment Failure

The seafloor sediment failures described here propagate downslope, triggered by initial loading by the volcanic debris avalanche. This contrasts with most large landslides on nonvolcanic continental margins, which are thought to often propagate retrogressively, by failing successive portions in an upslope direction. There are well-developed models of retrogressive landslide formation (Masson et al., 2010), but the physical mechanism driving downslope failure propagation is less clear, especially as such deformation can extend for tens of kilometers on very low (< 2°) gradients (Watt et al., 2012a; Figure 4). Although this style of landsliding is not well studied, it may be widespread in a range of settings (e.g., Trincardi and Normark, 1989). Because these types of failure remain confined (Frey-Martínez et al., 2006), they do not form prominent source scars or depositional morphologies, and thus may go unrecognized without the use of seismic reflection data.

Figure 6 presents a conceptual model for volcanic landslide emplacement that may drive downslope seafloor sediment failures (see Watt et al., 2012b). In the Montserrat example (Figure 5), there is a surficial deposit whose extent broadly matches that of the underlying deformation. We therefore envisage a coupled behavior, where translation of a relatively thin, overriding flow, perhaps triggered from the marginal portion of the debris avalanche, increases the pore-fluid pressure of the underlying sediment by preventing its drainage, and thus promotes continued downslope deformation. Such a process may be augmented (or entirely driven) by the propagation of a fracture along a basal surface (e.g., Viesca and Rice, 2010), which is consistent with the fact that the observed examples follow discrete basal stratigraphic horizons. Whether these horizons necessarily mark a layer with weak mechanical properties, which is countered by the fact that the basal surface steps up stratigraphy in places, or whether it is related to the depth of incision or erosion by the upslope debris avalanche (e.g., Figure 5A), remains unclear.

Formation of Debris Flows from Seafloor Sediment Failure

Offshore El Golfo, debris avalanche emplacement triggered the Canary debris flow, which had a runout of 600 km. This clearly distinguishes the Canary debris flow from the confined seafloor sediment failures discussed above (Figure 3b). However, the formation mechanisms may be comparable if the Canary debris flow represents a case where the seafloor sediment became disaggregated and escaped its source region rather than remaining confined within the region of initial disruption. The likelihood of evacuation and debris flow formation may relate to the depth of basal sediment failure surface, with deeper basal surfaces making it energetically more difficult to mobilize the sediment, and favoring the preservation of a confined landslide (see Frey-Martínez et al., 2006). Small differences in the gradient or extent of the seafloor slope may also affect the likelihood of transition to a debris flow, but this requires further investigation.

The Canary debris flow lacks a clear headwall, and certain features of the deposit are difficult to interpret. Masson et al. (1998) concluded that extensional fault scarps within the proximal part of the Canary debris flow, which extend into the region of debris-avalanche deposition (Figure 4), indicate that the debris flow formed while the debris avalanche (or components of it) was still moving. Continued motion of the avalanche may have enabled the initial seafloor sediment failure to disintegrate (Roberts and Cramp, 1996), while also obscuring the sources of failure in the proximal region. The areas affected by extensional faulting indicate that parts of the seafloor were deformed, but not

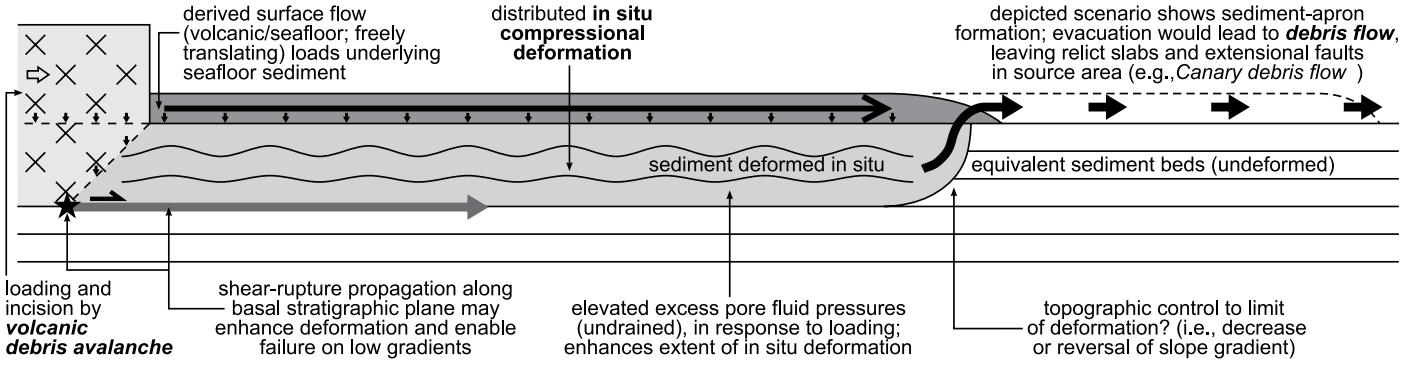

Figure 6. Schematic illustration of the potential mechanisms by which volcanic island landslides may form associated seafloor sediment failures.

mobilized, and this is also indicated by preserved relict slabs, which apparently lie in their original positions (Masson et al., 1998). The fault scarps themselves show increasing downslope erosion (Figure 4), perhaps caused by a turbidity current associated with the volcanic landslide. This set of observations suggests a complex co-evolution of the debris avalanche and debris flow deposits, potentially involving multiple phases of debris avalanche emplacement. As noted below, such multistage collapse behavior may be common.

Finally, it is instructive to consider a case where there is no evidence of debris-avalanche deposition triggering seafloor sediment failure, such as that of Montserrat's Deposit 1 (Figure 1). Here, the substrate was a fan of mixed volcanic debris accumulated from small mass flows (e.g., 0.1 km^3 or less), overlying a deeper debris-avalanche deposit. This coarse-grained and heterogeneous substrate was potentially more resistant to incision, more permeable, and thus less prone to the type of loading-induced sediment failure discussed above (Watt et al., 2012b). To generate failure of the substrate, a volcanic landslide may therefore need to be large enough to travel beyond the coarse volcanic sediment at the base of the island flanks into regions dominated by finer-grained, well-bedded sediment.

VOLCANIC LANDSLIDE FAILURE DYNAMICS AND TSUNAMI GENERATION

A key question for tsunami generation is whether volcanic island landslides occur in a single stage or multiple stages. If time gaps of even a few minutes separate discrete stages of failure, then the tsunami magnitude is reduced greatly (Løvholt et al., 2008). A simple model may assume a single failure event of one large block that undergoes fragmentation during transport. However, a range of observations argues against such a model. As noted above for the El Golfo landslide, it appears that debris-avalanche motion was contemporaneous with debris flow generation. The complex relationships between features of the El Golfo deposit and the Canary debris flow may partly arise from multiple stages of debris avalanche emplacement. The geometry of collapse chutes for a landslide such as Icod (Figure 1; Ablay and Hürlimann, 2000; Hunt et al., 2011) is also suggestive of multistage failure. A single intact block seems unlikely to fail on such an elongate failure plane; failure in multiple stages may be more likely, perhaps removing landslide portions retrogressively toward the final preserved headwall.

Evidence of Multistage Failure from Landslide-Triggered Turbidites

Grading patterns within landslide-generated turbidites provide strong evidence for multistage failures in the Canary Islands (Hunt et al., 2011, 2013b) and elsewhere (Garcia, 1996; Di Roberto et al., 2010; Watt et al., 2012b). For instance, turbidites associated with the Icod landslide comprise up to seven fining-up subunits, each deposited from a separate turbidity current (Figure 7). Pyroclastic grains within each subunit have distinct chemical compositions but have comparable size distributions, which precludes subunit deposition by complex flow patterns or sorting processes within a single turbidity current (Hunt et al., 2011). This interpretation is supported by the morphology of the main Icod landslide deposit, whose banked surface defines several overlapping lobes (Ablay and Hürlimann, 2000). The initial three Icod turbidite subunits have abundant calcareous grains and altered volcanic grains, suggesting that the initial stages of failure involved the submerged island flanks. These initial stages also dominate (> 65%) the total landslide volume. It thus appears that failure was retrogressive and that successive stages decreased in volume. Hunt et al. (2013b) use a similar approach to show that seven other landslides in the Canary Islands occurred in multiple stages (Figure 7). Multistage landslide emplacement should now be considered in models of tsunami generation from volcanic island landslides.

CONCLUSIONS

The characteristics of volcanic-island landslide deposits, which include the presence of extensive volumes of seafloor sediment and emplacement dynamics that occur in multiple stages, have implications for hazard generation from such events. A full understanding of this hazard requires information about the magnitude and frequency of past landslides and the way in which they were formed. Seismic reflection profiles are required to understand the true nature of landslide deposits around volcanic islands because an interpretation based on surface morphology alone may misidentify both the number and magnitude of past events. It is also particularly important to distinguish between failed material from the volcanic edifice and from the surrounding seafloor. Seafloor sediment failures of the type discussed here are likely to have a low capacity for tsunami generation. The volume of the volcanic failure is a more significant factor for the generation of damaging tsunamis (see Watt et al., 2012a). The occurrence of volcanic failure in multiple stages substantially reduces the potential for ocean-wide impacts. The magnitude,

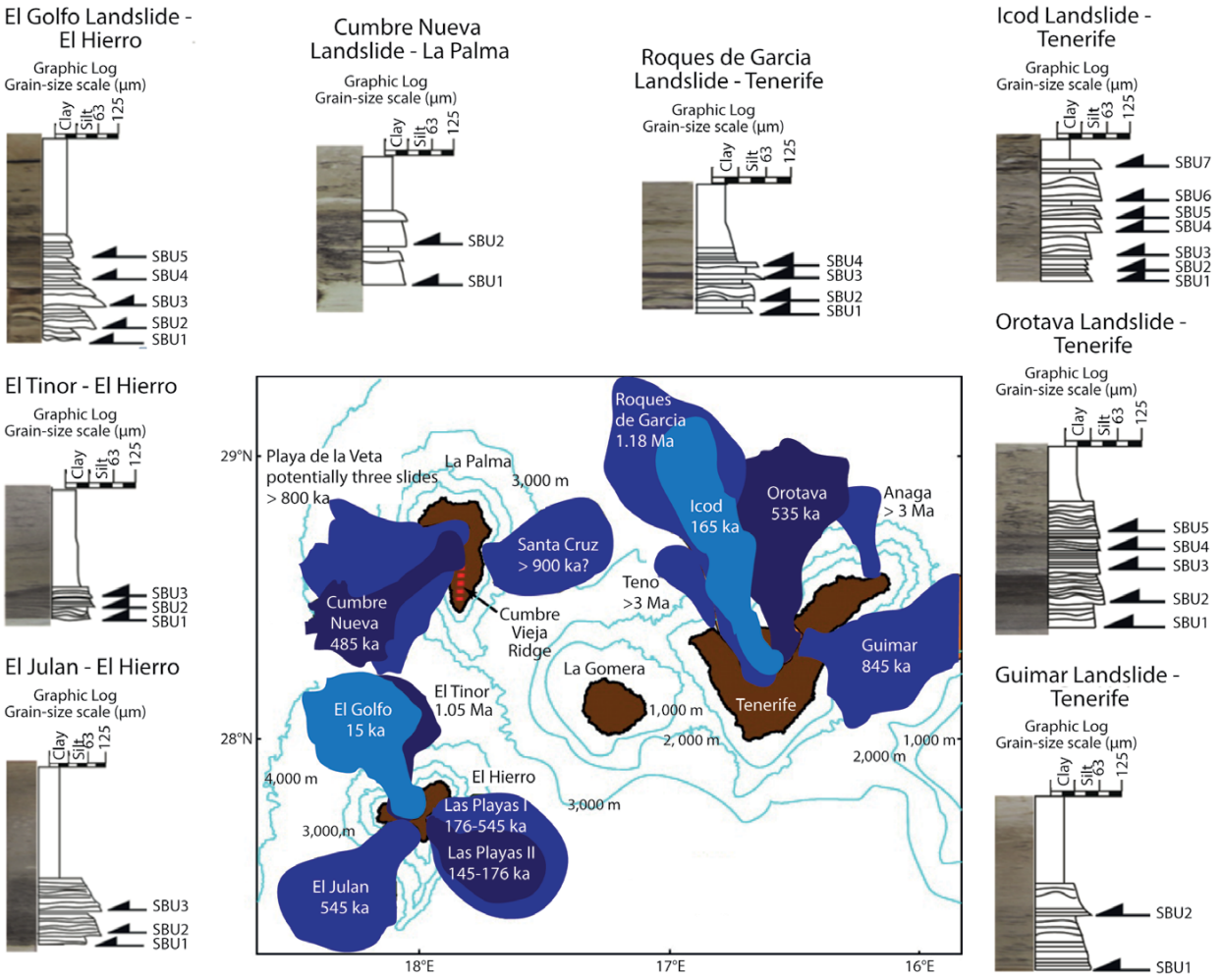

Figure 7. Summary map of landslide deposits around the Canary Islands showing turbidite stratigraphies generated by these events. Each turbidite comprises multiple graded beds, indicating multistage failure of the parental landslide. For full site details, see Hunt et al. (2013a).

dynamics, and impacts of volcanic island landslides are not readily assessed from the final landslide deposit without a good understanding of the components that make up the deposit.

ACKNOWLEDGMENTS

We are grateful to Neil Mitchell and Michelle Coombs for detailed reviews, and acknowledge research funding from the UK Natural Environment Research Council (NE/I02044X/1).

REFERENCES

Ablay, G., and M. Hürlimann. 2000. Evolution of the north flank of Tenerife by recurrent giant landslides. *Journal of Volcanology and Geothermal Research* 103:135–159, http://dx.doi.org/10.1016/S0377-0273(00)00220-1.

Boulesteix, T., A. Hildenbrand, P.-Y. Gillot, and V. Soler. 2012. Eruptive response of oceanic islands to giant landslides: New insights from the geomorphologic evolution of the Teide-Pico Viejo volcanic complex (Tenerife, Canary). *Geomorphology* 138:61–73, http://dx.doi.org/10.1016/j.geomorph.2011.08.025.

Coombs, M.L., S.M. White, and D.W. Scholl. 2007. Massive edifice failure at Aleutian arc volcanoes. *Earth and Planetary Science Letters* 256:403–418, http://dx.doi.org/10.1016/j.epsl.2007.01.030.

Crandell, D.R. 1989. *Gigantic Debris Avalanche of Pleistocene Age from Ancestral Mount Shasta Volcano, California, and Debris-Avalanche Hazard Zonation*. US Geological Survey Bulletin 1861, 32 pp, http://pubs.usgs.gov/bul/1861/report.pdf.

Delcamp, A., B. van Wyk de Vries, and M.R. James. 2008. The influence of edifice slope and substrata on volcano spreading. *Journal of Volcanology and Geothermal Research* 177:925–943, http://dx.doi.org/10.1016/j.jvolgeores.2008.07.014.

Deplus, C., A. Le Friant, G. Boudon, J.C. Komorowski, B. Villemant, C. Harford, J. Ségoufin, and J.L. Cheminée. 2001. Submarine evidence for large-scale debris avalanches in the Lesser Antilles Arc. *Earth and Planetary Science Letters* 192:145–157, http://dx.doi.org/10.1016/S0012-821X(01)00444-7.

Di Roberto, A., M. Rossi, A. Bertagnini, M.P. Marani, and F. Gamberi. 2010. Distal turbidites and tsunamigenic landslides of Stromboli Volcano (Aeolian Islands, Italy). Pp. 719–732 in *Submarine Mass Movements and Their Consequences*. D.C. Mosher, R.C. Shipp, L. Moscardelli, J.D. Chaytor, C.D.P. Baxter, H.J. Lee, and R. Urgules, eds, Advances in Natural and Technological Hazards Research vol. 28, Springer.

Frey-Martínez, J., J. Cartwright, and D. James. 2006. Frontally confined versus frontally emergent submarine landslides: A 3D seismic characterisation. *Marine and Petroleum Geology* 23:585–604, http://dx.doi.org/10.1016/j.marpetgeo.2006.04.002.

Fritz, H.M., W.H. Hager, and H.E. Minor. 2004. Near field characteristics of landslide generated impulse waves. *Journal of Waterway, Port, Coastal, and Ocean Engineering* 130:287–302, http://dx.doi.org/10.1061/(ASCE)0733-950X(2004)130:6(287).

Garcia, M.O. 1996. Turbidites from slope failure on Hawaiian volcanoes. *Geological Society, London, Special Publications* 110:281–294, http://dx.doi.org/10.1144/GSL.SP.1996.110.01.22.

Glicken, H. 1996. *Rockslide-Debris Avalanche of May 18, 1980, Mount St. Helens Volcano*. US Geological Survey Open-File Report 96-677, http://vulcan.wr.usgs.gov/Projects/Glicken/framework.html.

Hunt, J.E., R.B. Wynn, D.G. Masson, P.J. Talling, and D.A.H. Teagle. 2011. Sedimentological and geochemical evidence for multistage failure of volcanic island landslides: A case study from Icod landslide on north Tenerife, Canary Islands. *Geochemistry, Geophysics, Geosystems* 12, Q12007, http://dx.doi.org/10.1029/2011GC003740.

Hunt, J.E., R.B. Wynn, P.J. Talling, and D.G. Masson. 2013a. Turbidite record of frequency and source of large volume (> 100 km^3) Canary Island landslides in the last 1.5 Ma: Implications for landslide triggers and geohazards. *Geochemistry, Geophysics, Geosystems* 14:2,100–2,123, http://dx.doi.org/10.1002/ggge.20139.

Hunt, J.E., R.B. Wynn, P.J. Talling, and D.G. Masson. 2013b. Multistage collapse of eight western Canary Island landslides in the last 1.5 Ma: Sedimentological and geochemical evidence from subunits in submarine flow deposits. *Geochemistry, Geophysics, Geosystems* 14:2,159–2,181, http://dx.doi.org/10.1002/ggge.20138.

Iverson, R.M. 1997. The physics of debris flows. *Reviews of Geophysics* 35:245–296, http://dx.doi.org/10.1029/97RG00426.

Le Friant, A., G. Boudon, C. Deplus, and B. Villemant. 2003. Large-scale flank collapse events during the activity of Montagne Pelée, Martinique, Lesser Antilles. *Journal of Geophysical Research* 108:1,978–2,012, http://dx.doi.org/10.1029/2001JB001624.

Løvholt, F., G. Pedersen, and G. Gisler. 2008. Oceanic propagation of a potential tsunami from the La Palma Island. *Journal of Geophysical Research* 113, C09026, http://dx.doi.org/10.1029/2007JC004603.

Manconi, A., M.A. Longpré, T.R. Walter, V.R. Troll, and T.H. Hansteen. 2009. The effects of flank collapses on volcano plumbing systems. *Geology* 37:1,099–1,102, http://dx.doi.org/10.1130/G30104A.1.

Masson, D.G., M. Canals, B. Alonso, R. Urgeles, and V. Hühnerbach. 1998. The Canary debris flow: Source area morphology and failure mechanisms. *Sedimentology* 45:411–432, http://dx.doi.org/10.1046/j.1365-3091.1998.0165f.x.

Masson, D.G., A.B. Watts, M.J.R. Gee, R. Urgeles, N.C. Mitchell, T.P. Le Bas, and M. Canals. 2002. Slope failures on the flanks of the western Canary Islands. *Earth-Science Reviews* 57:1–35, http://dx.doi.org/10.1016/S0012-8252(01)00069-1.

Masson, D.G., T. Le Bas, I. Grevemeyer, and W. Weinrebe. 2008. Flank collapse and large-scale landsliding in the Cape Verde Islands, off West Africa. *Geochemistry, Geophysics, Geosystems* 9:Q07015, http://dx.doi.org/10.1029/2008GC001983.

Masson, D.G., R.B. Wynn, and P.J. Talling. 2010. Large landslides on passive continental margins: Processes, hypotheses and outstanding questions. Pp. 153–165 in *Submarine Mass Movements and Their Consequences*. D.C. Mosher, R.C. Shipp, L. Moscardelli, J.D. Chaytor, C.D.P. Baxter, H.J. Lee, and R. Urgules, eds, Advances in Natural and Technological Hazards Research vol. 28, Springer.

Mazzanti, P., and F. De Blasio. 2013. The dynamics of subaqueous rock avalanches: The role of dynamic fragmentation. Pp. 35–40 in *Landslide Science and Practice*, vol. 5. C. Margottini, P. Canuti, and K. Sassa, eds, Springer-Verlag Berlin Heidelberg.

McGuire, W.J. 1996. Volcano instability: A review of contemporary themes. *Geological Society, London, Special Publications* 110:1–23, http://dx.doi.org/10.1144/GSL.SP.1996.110.01.01.

Mitchell, N.C. 2003. Susceptibility of mid-ocean ridge volcanic islands and seamounts to large-scale landsliding. *Journal of Geophysical Research* 108:1,978–2,012, http://dx.doi.org/10.1029/2002JB001997.

Montanaro, C., and J. Beget. 2011. Volcano collapse along the Aleutian Ridge (western Aleutian Arc). *Natural Hazards and Earth System Sciences* 11:715–730, http://dx.doi.org/10.5194/nhess-11-715-2011.

Moore, J.G., and D.A. Clague. 2002. Mapping the Nuuanu and Wailau landslides in Hawaii. Pp. 223–244 in *Hawaiian Volcanoes: Deep Underwater Perspectives*. E. Takahashi, P.W. Lipman, M.O. Garcia, J. Naka, and S. Aramaki, eds, American Geophysical Union, Washington, DC, http://dx.doi.org/10.1029/GM128p0223.

Moore, J.G., D.A. Clague, R.T. Holcomb, P.W. Lipman, W.R. Normark, and M.E. Torresan. 1989. Prodigious submarine landslides on the Hawaiian ridge. *Journal of Geophysical Research* 94:17,465–17,484, http://dx.doi.org/10.1029/JB094iB12p17465.

Naranjo, J.A., and P. Francis. 1987. High velocity debris avalanche at Lastarria volcano in the north Chilean Andes. *Bulletin of Volcanology* 49:509–514, http://dx.doi.org/10.1007/BF01245476.

Nishimura, Y. 2008. Volcanism-induced tsunamis and tsunamiites. Pp. 163–184 in *Tsunamiites: Features and Implications*. T. Shiki, Y. Tsuji, K. Minoura, and T. Yamazaki, eds, Elsevier.

Pinel, V., and F. Albino. 2013. Consequences of volcano sector collapse on magmatic storage zones: Insights from numerical modeling. *Journal of Volcanology and Geothermal Research* 252:29–37, http://dx.doi.org/10.1016/j.jvolgeores.2012.11.009.

Roberts, J.A., and A. Cramp. 1996. Sediment stability on the western flanks of the Canary Islands. *Marine Geology* 134:13–30, http://dx.doi.org/10.1016/0025-3227(96)00021-7.

Siebe, C., J.C. Komorowski, and M.F. Sheridan. 1992. Morphology and emplacement of an unusual debris-avalanche deposit at Jocotitlán volcano, Central Mexico. *Bulletin of Volcanology* 54:573–589, http://dx.doi.org/10.1007/BF00569941.

Siebert, L. 1984. Large volcanic debris avalanches: Characteristics of source areas, deposits, and associated eruptions. *Journal of Volcanology and Geothermal Research* 22:163–197, http://dx.doi.org/10.1016/0377-0273(84)90002-7.

Silver, E., S. Day, S. Ward, G. Hoffmann, P. Llanes, N. Driscoll, B. Appelgate, and S. Saunders. 2009. Volcano collapse and tsunami generation in the Bismarck Volcanic Arc, Papua New Guinea. *Journal of Volcanology and Geothermal Research* 186:210–222, http://dx.doi.org/10.1016/j.jvolgeores.2009.06.013.

Talling, P.J., D.G. Masson, E.J. Sumner, and G. Malgesini. 2012. Subaqueous sediment density flows: Depositional processes and deposit types. *Sedimentology* 59:1,939–2,003, http://dx.doi.org/10.1111/j.1365-3091.2012.01353.x.

Tinti, S., G. Pagnoni, and F. Zaniboni. 2006. The landslides and tsunamis of the 30th of December 2002 in Stromboli analysed through numerical simulations. *Bulletin of Volcanology* 68:462–479, http://dx.doi.org/10.1007/s00445-005-0022-9.

Trincardi, F., and W.R. Normark. 1989. Pleistocene Suvero slide, Paola basin, southern Italy. *Marine and Petroleum Geology* 6:324–335, http://dx.doi.org/10.1016/0264-8172(89)90029-9.

Viesca, R.C., and J.R. Rice. 2010. Modeling slope instability as shear rupture propagation in a saturated porous medium. Pp. 215–225 in *Submarine Mass Movements and Their Consequences*. D.C. Mosher, R.C. Shipp, L. Moscardelli, J.D. Chaytor, C.D.P. Baxter, H.J. Lee, and R. Urgules, eds, Advances in Natural and Technological Hazards Research vol. 28, Springer.

Wadge, G., P.W. Francis, C.F. Ramirez. 1995. The Socompa collapse and avalanche event. *Journal of Volcanology and Geothermal Research* 66:309–336, http://dx.doi.org/10.1016/0377-0273(94)00083-S.

Ward, S.N. 2001. Landslide tsunami. *Journal of Geophysical Research* 106:11,201–11,215, http://dx.doi.org/10.1029/2000JB900450.

Ward, S.N., and S. Day. 2003. Ritter Island volcano—Lateral collapse and the tsunami of 1888. *Geophysical Journal International* 154:891–902, http://dx.doi.org/10.1046/j.1365-246X.2003.02016.x.

Watt, S.F.L., P.J. Talling, M.E. Vardy, V. Heller, V. Huhnerbach, M. Urlaub, S. Sarkar, D.G. Masson, T.J. Henstock, T.A. Minshull, and others. 2012a. Combinations of volcanic-flank and seafloor-sediment failure offshore Montserrat, and their implications for tsunami generation. *Earth and Planetary Science Letters* 319:228–240, http://dx.doi.org/10.1016/j.epsl.2011.11.032.

Watt, S.F.L., P.J. Talling, M.E. Vardy, D.G. Masson, T.J. Henstock, V. Huhnerbach, T.A. Minshull, M. Urlaub, E. Lebas, A. Le Friant, and others. 2012b. Widespread and progressive seafloor-sediment failure following volcanic debris avalanche emplacement: Landslide dynamics and timing offshore Montserrat, Lesser Antilles. *Marine Geology* 323–325:69–94, http://dx.doi.org/10.1016/j.margeo.2012.08.002.